ISSN 1027-5495. Functional Materials, 30, No.3 (2023), p. 413-423.
doi:https://doi.org/10.15407/fm30.03.413

Mutual impact of alternative mechanisms of a dopant embedding into an ordered medium: a case of gramicidin S in model lipid membranes

***R.Ye.Brodskii*[1], *O.V.Vashchenko*[2]**

[1]Institute for Single Crystals, National Academy of Science of Ukraine, 60 Nauky Ave., 61072 Kharkiv, Ukraine
[2]Institute for Scintillation Materials, National Academy of Science of Ukraine, 60 Nauky Ave., 61072 Kharkiv

Received May 25, 2023

Governing mechanisms of dopants interactions with host media are of peculiar importance in the light of development of novel materials. Lipid structures, including bilayer membranes, are vivid examples of ordered media with plenty ways of practical usage. In this work, *L*-α-dipalmitoylphosphatidylcholine (DPPC) membrane doped with an antimicrobial peptide gramicidin S (GS) is under consideration. Due to GS ability to form associates inside the membrane, this is a case when the same dopant behaves like two different ones, whereby lipid shells around GS monomers and associates porly mix with one another and lipid domains of two different types arise. Data of differential scanning calorimetry (DSC) were collected reflecting phase transitions in the system. Some unusual GS features were observed by means of DSC. In particular, a power-law concentration dependence of phase transition temperature was obtained for monomer-containing domains, where the exponent is higher than 1, which is rather typical for polymolecular sorption. We proposed a phenomenological model based on mutual impact of alternative mechanisms of 'dopant - medium' interactions. Within the framework of the model, the system DPPC + GS is considered as two-dimension nano-emulsion composed of two different types of domains where processes on the domains boundaries, including generation of free volume, affecting significantly the system properties. The model allows us to explain quite well a number of membranotropic features of GS, including its antimicrobial action, and could be useful for interpretation and prediction of GS effects in various model and cell membranes.

Keywords: model lipid membrane, gramicidin S, phenomenological model, mechanisms of dopants action, mutual impact, differential scanning calorimetry.

Взаємний вплив альтернативних механізмів вбудовування допанта у впорядковане середовище: випадок граміцидину S у модельній ліпідній мембрані. *Р.Є.Бродський, О.В.Ващенко*

Механізми, що керують взаємодією допантів з середовищем є об'єктами особливої уваги при розробці нових матеріалів. Ліпідні структури, зокрема бішарові мембрани, є яскравими прикладами впорядкованих середовищ, які мають чимало шляхів практичного застосування. В даній роботі розглянуто мембрани *L*-α-діпальмітоїлфосфатидилхоліну (ДПФХ), доповані антимікробним пептидом граміцидином S (ГС). Завдяки здатності ГС утворювати асоціати всередині мембрани у цьому випадку один й той самий допант відіграє роль двох різних, оскільки ліпідні оболонки, що формуються навколо мономерів ГС та його асоціатів, змішуються між собою, утворюючи ліпідні домени двох різних типів. Отримано дані диференціальної скануючої калориметрії (ДСК), які відбивають фазові переходи у системі. На основі даних ДСК виявлено низку незвичайних

властивостей ГС. Зокрема, степенева концентраційна залежність температури фазового переходу доменів, які містять мономери ГС, характеризується значенням ступеню більше 1, що характерно для полімолекулярної сорбції. У роботі запропоновано феноменологічну модель на основі взаємного впливу альтернативних механізмів взаємодії допанта та середовища. В рамках цієї моделі система ДПФХ + ГС розглядається як двовимірна двофазна наноемульсія, складається з двох типів доменів, у якій велике значення мають процеси на межах доменів, зокрема генерація вільного об'єму. Модель дозволяє пояснити низку мембранотропних властивостей ГС, у тому числі його антимікробну активність, та може бути корисною при інтерпретації та прогнозуванні ефектів ГС у різних модельних та клітинних мембранах.

1. Introduction

Lipid membranes are very sophisticated and interesting examples of ordered media with plenty ways of practical usage, including pharmacology, cosmetology, ecology, food industry, etc. Fundamental investigations involving lipid membrane allow one to reveal and/or to refine mechanisms of membranotropic action of various drugs. In the case of antimicrobial peptides, which are widely regarded as prospective substitutes of conventional antibiotics, poor understanding of the action mechanisms is one of the major obstacles that have slowed progress in this field [1]. One of the most prospective antimicrobial peptides is gramicidin S (GS), which remains effective over 80 years since its discovery [2].

It was established that antibacterial action of GS is directly related to damages of lipid membranes of bacterial cells under GS sorption [3]. Numerous experiments showed that such damages result in significant elevation of the membrane permeability and eventually to cell death. However, specific mechanism of the phenomena depends on many factors such as the 3D conformation of the molecule, its physical properties and the actual interactions with the lipids [1]. Nowadays, two main mechanisms are considered for antimicrobial peptide action, namely, pore formation or carpet formation [1, 4]. Additionally, the mechanism of curvature changes is considered for some peptides, which concerns formation of non-lamellar phase [1, 5]. Also, there is another mechanism of membrane permeabilizing, which is related to higher lipid heterogeneity within lamellar phase [6]. Below we will consider realization of this mechanism in the case of GS.

For a long time, it was believed that GS disturbs membrane integrity by the pore formation mechanism [7, 18]. Indeed, this mechanism was established for its close analogues, gramicidin A and gramicidin D, which, however, possess quite different molecular structures [8]. In the case of GS, direct confirmation of pore formation has still not been obtained. On the contrary, some novel data indicate that an alternative mechanism might take place. Indeed, in bacterial membrane *in vivo* no pore formation was established, instead, significant changes in lipid packing takes place, including formation of large liquid crystalline domains [9–12]. So, the molecular mechanism of GS action is still not completely clear.

In order to shed some light to the matter, one first should be acquainted with some peculiarities of GS–membrane interaction. A number of work reports that monomeric GS molecules (GSM) are able to aggregate in membrane medium [4, 13]. This phenomenon was initially called oligomerization [4], but since no covalent bonds form under such aggregation, it seems more correctly to refer these formations as GS associates (GSA). Here, it should be noted that all investigations of GSA concern solely membrane medium and no mention of GSA formation in any liquid phases (water, ethanol, etc.) was found.

Localization of GSM and GSA in lipid membranes significantly differs [4, 14–16]. GSM localize in hydrophilic parts of membrane, directly above its surface, with its charged side-groups oriented to the side of water phase. GSA locate, on the contrary, in the hydrophobic interior of membrane and are oriented perpendicular to the membrane surface. So, GSA formation is coupled with molecules re-alignment [4]. As it was suggested in [13], GSA form certain rounded structure with a pore inside. However, sufficient lateral pressure of lipid hydrocarbon moieties GSA seems factor which should prevent such loose package.

GSA effect on lipid membranes is obviously differs from GSM effect, so one can talk about two-modal character of GS–membrane interactions due to its two-modal distribution. Such type of distribution (caused by aggregation of the molecules) is known for a number of dopants and it is noted that the second mode appears above a certain threshold concentration [8, 17]. As for GS,

a two-site model was proposed for its binding with L-α-dipalmitoylphosphatidylcholine (DPPC) membrane, which is accompanied by endothermic effect [18], i.e. it is entropy-driven. It was also established that second mode is characterized by certain threshold concentration, so it could be attributed to GSA binging [18]. This binding constant is 2–3 orders of magnitudes smaller than GSM binding and depends on membrane lipid composition. The threshold GS concentration was estimated as 2 to 2.5 mol % in different membranes [4, 15] (for comparison, saturation shell in DPPC membrane was estimated as 20 mol % [15]).

For the above mentioned gramicidin A and gramicidin D, two-modal distribution was also shown in dimyristoylphosphatidylcholine membrane, and it is remarkable that gramicidin monomers are randomly distributed over the membrane whereas gramicidin dimers are regularly distributed, in some cases, even to superlattices [17].

Under investigation of GS derivatives, it was established that lowering of their amphipathicity (hydrophobicity elevation) correlates with increase in their antimicrobial activity, whereas diminishing of the amphipathicity reflects in increasing of their lytic activity [19]. So, it was suggested that different modes of GS binding could be responsive for its different effects [4].

Generally, GS binding to lipid membrane was found to be dependent on membrane properties. In particular, GS sorption is higher for membranes with higher fluidity and lower lipid ordering [15]. It is also known GSA formation is facilitated under membrane phase transition [4].

Thus, a number of facts and assumptions have been accumulated by now concerning GS–membrane interaction. Some of them are consistent with each other, but many other seem controversial. In the present work, an attempt was made to summarize and agree some literature and our own experimental data within the framework of the proposed theory of mutual impact of alternative mechanisms of a dopant embedding in membrane medium.

2. Materials and methods

2.1. Membrane preparation

Chemically pure L-α-dipalmitoylphosphatidylcholine (DPPC) was purchased from "Sigma- Aldrich". Gramicidin S (GS) manufactured by "Renewal" Ltd. was used after additional purification. The procedure of model lipid membrane preparation included solvation of GS and DPPC with a proper amount of ethanol, thorough solvent evaporation using a concentrator Concentrator Plus ("Eppednorf") and following hydration of the samples with Hanks balanced salt solution without phenol red (HBSS), pH 7.4 ("Thermo Fisher Scientific"). Hydrated samples were incubated for 4–5 days at 5°C, with several heatings up to 50°C combined with careful mixing. GS concentration in the system was varied from 1 to 8 mol %; water content was kept 60 % wt/wt relative to the dry fraction.

2.2. Calorimetric investigations

Differential scanning calorimetry (DSC) studies were performed using a microcalorimeter Mettler DSC1 ("Mettler-Toledo"). A sample (ab. 15 mg) was placed into a standard 40 μl aluminum crucible which was immediately sealed with a lid. DSC profiles of the samples were obtained in the temperature range 20 to 50°C with scanning rate 1 K/min.

Shift of melting peaks, $|\Delta T|$, and peak asymmetry, a, were determined from the obtained DSC profiles as:

$$|\Delta T| = |T_m - T_m^0|, \quad (1)$$

$$a = T_m - T_m^c, \quad (2)$$

where T_m is the temperature of peak maximum for the system under investigation; T_m^0 is the temperature of peak maximum for undoped DPPC membrane; T_m^c is the peak centroid.

Peak deconvolution procedure was performed using free software QtiPlot [20]. Coefficient of determination R^2 between the original curve and the envelope was higher than 0.99 in all cases examined.

3. Differential scanning calorimetry data

By means of DSC techniques, a set of thermograms was obtained which reflect phase transition "gel-liquid crystal" (also called membrane melting) for DPPC membrane containing 1 to 8 mol % of GS. Her it should be noted that the concentrations used are far from saturation threshold (20 mol % [15]). In Fig. 1, some parameters of phase transitions are presented as a function of GS concentration (the procedure of their obtaining form original DSC data is described in Sec. 2.2). As one can see, the peak temperature (T_{peak}) lowers with GS concentration, whereas the peak asymmetry

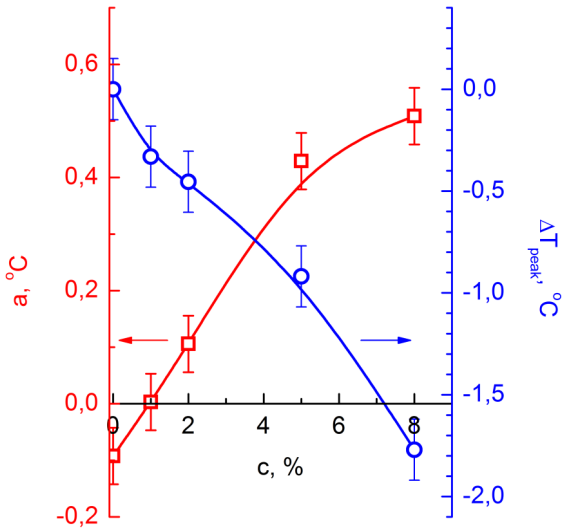

Fig. 1. Shift of membrane melting temperature (the right axis) and the peak asymmetry changes (the left axis) in DPPC membrane containing GS.

(a) elevates. The former indicates the appearance of some low-temperature component of the DSC peak. The fraction of this component grows monotonously with GS content. Taking into account two-modal GS distribution into lipid membranes, one could assume that this low-temperature component corresponds to the appearance of GSA in the system. Thus, two types of lipid shells (surrounding GSA or GSM) are substantially different and form GSA-containing and GSM-containing lipid domains, respectively.

Basing on the foregoing, it seems reasonable to decompose the original DSC peak into two components (see Sec. 2.2 for details). Some parameters of the obtained peaks, namely, the absolute shift of melting temperature ($|\Delta T|$) and the peak half-width ($\Delta T^{1}_{m}/_{2}$), are presented in Fig. 2. For $|\Delta T|(c)$ dependences, approximation was performed basing on Freundlich adsorption equation [21]. This adsorption model is commonly applied to adsorption in various media in the middle range of concentrations of adsorbent. Here, we use this equation in the following form [22]:

$$|\Delta T| = bc^{\gamma}, \qquad (3)$$

where c is the dopant concentration, b and γ are phenomenological constants. Here, b formally determines $|\Delta T|$ value for unit dopant concentration and γ characterizes the sorption process.

In Fig. 2, one could note essential difference in the shape of $|\Delta T|(c)$ dependences

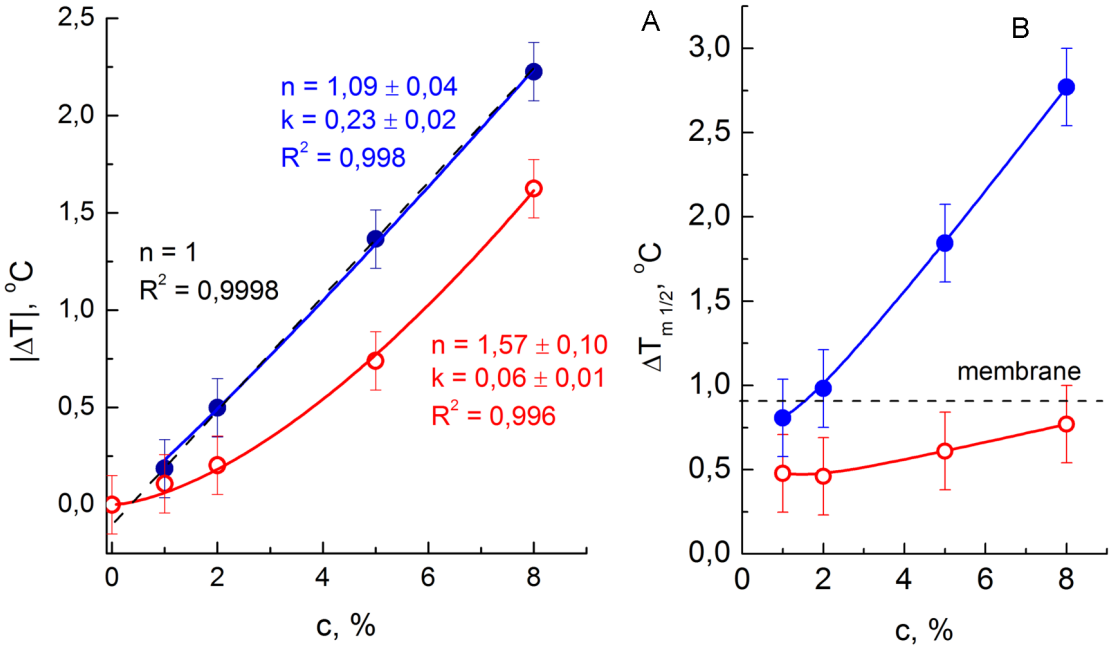

Fig. 2. Panel A: Shift of DSC peaks maximum of GSM-containing domains (open symbols) and GSA-containing domains (solid symbol) depending on GS content in the system (c). Parameters of approximations by Freundlich adsorption equation (Eq. 3) and linear equation are presented together with their coefficients of determination R2. Panel B: Corresponding changes of DSC peak halfwidth ($\Delta T_{m}{}^{1}/_{2}$. Dotted line points the value of $\Delta T_{m}{}^{1}/_{2}$ for the undoped DPPC membrane.

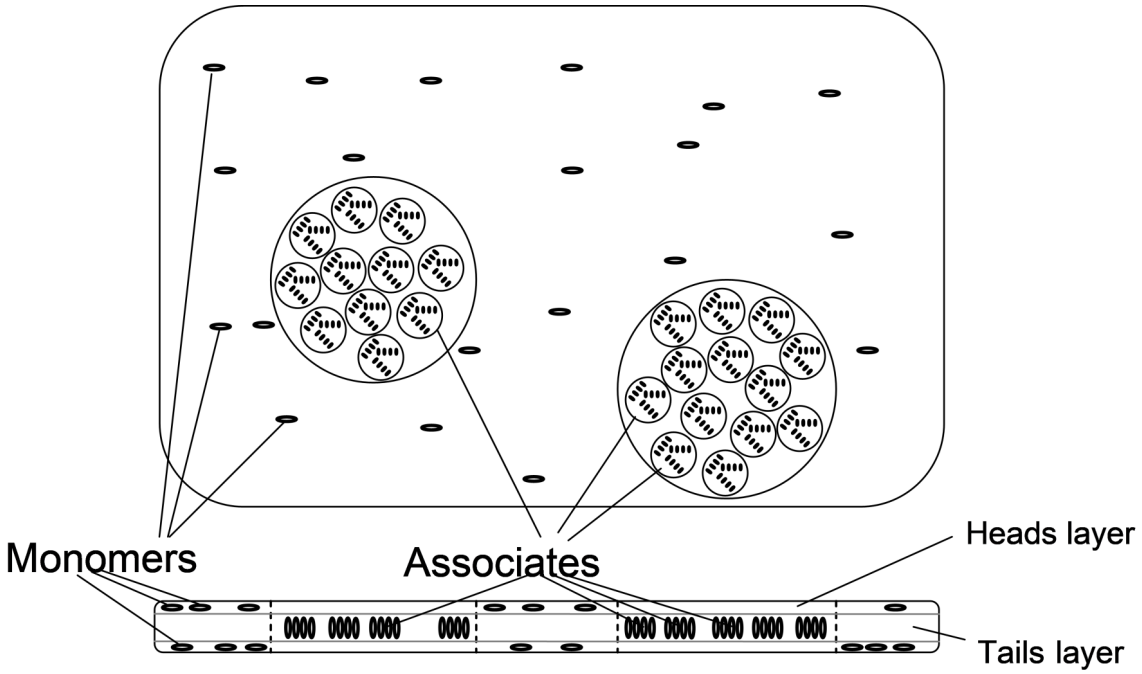

Fig. 3. A scheme of GS monomers and associates location in the lipid membrane. The upper figure depicts the top view; the lower figure is the side view (parallel to the membrane surface).

for GSM-containing and GSA-containing domains. Indeed, for GSA-containing domains $\gamma \approx 1$, which reflects linear proportionality between the amount of GS associates bonded to the membrane and total GS concentration in the system. At the same time, for the GSM-containing domains, $\gamma \approx 1.6$, which formally means that distribution of GSM into the membranes increases much stronger than total GS concentration. Such features are generally typical for polymolecular sorption, but there seem no obvious reasons for it in the system studied. The values of DSC peak half-width, $\Delta T_{m^1/2}$, reveals further distinctions between the two types of domains. Indeed, $\Delta T_{m^1/2}$ for the GSM-containing domains is close to the corresponding value for the undoped membrane and remains almost unchanged with GS concentration. On the contrary, $\Delta T_{m^1/2}$ of the GSA-containing domains rises significantly (see Fig. 2, B). These features are in line with data [23] concerning a decrease in the degree of cooperativity of the main phase transition and increase in the volume compressibility of the vesicles under GS doping.

Thus, GS binding to DPPC membrane results in formation of two different lipid fractions. None of them is pure membrane, which indicates sufficient GS solubility in the membrane. These domains do not mix together and actually form a kind of emulsion "membrane in membrane" (Fig. 3). A physical reason of this phenomena could be the essential difference in lipid ordering and energy of lipid-lipid interactions between GSM and GSA lipid shells. Such heterogeneous system obviously has a larger amount of phase boundaries. Increase in lipid package heterogeneity is an appropriate reason of elevation of the membrane permeability [6], so GS antimicrobial action could be a direct consequence of GS-induced non-homogeneity in lipid packing.

Further, the threshold GS concentration (see Sec. 1) seems to be the threshold of lipid phase separation. Under high GS content, the GSM peak disappears completely (data are not shown). In our opinion, it indicates either that the GSA phase distributes over the whole membrane or that picture becomes the opposite of the initial, namely, GSM content is insufficient to form a separate phase with its own lipid ordering and phase transition temperature.

Besides, the ability of GS to form lipid domains with different properties could be directly related to their biological activity. It is known [24] that some membrane compartments are able to have affinity to the same type of lipid domains, so in the case of phase separation they would appear closer to each other and their interaction could be facilitated. At the same time, the compartments with affinity to different domains

would be segregated one from another and their interaction could be disturbed. Thus, GS effect may also affect cell interactions with another drugs, especially with membranoactive ones.

Returning to the mechanisms of GS membranotropic effects, we could see two featrues of the phenomenon observed:

(1) free volume generation which is formally indicated from the value $\gamma > 1$ (Eq. 3); as it was shown in [25], it could be a driving factor in this case;

(2) conjunction (mutual impact) of GSM and GSA sorption into the membrane.

Generally, one can see that indirect hydrophilic-hydrophobic interactions occur in the system studied consisting in mutual impact between dopant-induced modifications in hydrophilic and hydrophobic parts of the membrane.

4. Molecular visualization

Building of molecular models was performed by means of free software Chemdraw 3d [26] using MM2 optimization in vacuum interior. The results suggest that GS molecules are able to form tight associate by stacking mechanism, with no tendency to pore formation (Fig. 4). The estimated GSA width is ab. 20 Å, which corresponds to the length of GS molecule and is in accordance with [4]. GSA seem to be stabilized not only by hydrogen bonds [4], but also by electrostatic and hydrophilic-hydrophobic interactions with hydrophilic ornithine residues to be oriented inside a GSA.

Localization of GSA inside the non-polar membrane interior requires an increase in its hydrophobicity (i.e. decrease in hydrophilicity) comparing to the monomers. To achieve this effect, hydrophilic side radicals of GS molecules should to be inside GSA. In the simplest case (GSA containing two monomers) these radicals are turned towards each other (see Fig. 3). However, there are no steric hindrances for these radicals to be turned in different directions, in such a way that monomers could be strung on top of each other like beads. As a result, tight molecular packing takes place, without pore formation and any internal restriction to GSA growth. Following to this scheme of the GSA grows inside the membrane, the width of the associate remains unchanged, with growth only in its length. Such structure fits quite well to the thickness of the membrane interior, and its growth is only hindered by accessible space into the membrane. However, further detailed molecular modelling is obviously necessary.

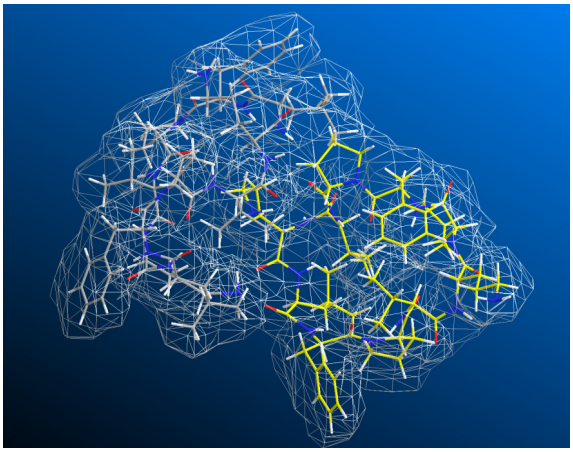

Fig. 4. GS associate formed by two monomers.

The above reasoning allows one to conclude that GSA could be formed rather in membrane medium than in water phase. Indeed, if the GSA are less polar than the monomers, their content in water would be much less than in the membrane. So, the first mode of GS binding would be monomer adsorption, and associate formation would be the second one, in full compliance with numerous literature data.

5. Theory

5.1. Unusual membranotropic effects of GS

Basing on the obtained experimental data concerning DPPC membrane containing GS, one can highlight a number of unusual effects to be explained.

1. Splitting of the original DSC peak of the membrane phase transition into two ones, still none of them follows the canonical Freundlich adsorption equation, where γ should be less than 1, but generally follows Eq. (3).

2. Linear dependence $|\Delta T|(c)$ for the peak corresponding to higher values of $|\Delta T|$ (GSA-containing domains).

3. Power-law dependence with the exponent higher 1 for the peak corresponding to lower values of $|\Delta T|$ (GSM-containing domains).

The appearance of two DSC peaks of membrane melting in the presence of GS is obviously a sign that the membrane separates into lipid domains with different properties, including melting temperatures [27–31]. The basic cause of these phenomena is the two-modal character of GS distribution into membrane reported in literature (see Sec. 1). Indeed, a part of GS in monomeric form is adsorbed at the hydrophilic membrane

surface whereas another part is able to form associates and to penetrate into the hydrophobic inner part of the membrane. It seems reasonable that the number of GS molecules in the associate could be determined, inter alia, by membrane properties. Lipid package and interactions in GSM and GSA lipid shells are so different that their mixing becomes energetically unfavorable. So, different types of lipid shells tend to separate for reducing phase boundaries. Thus, different lipid microdomains are formed and membrane becomes emulsified (Fig. 4).

Detailed analysis of literature and our own experimental data (see Secs. 1 and 4) allowed us to conclude that the peak with lower values of $|\Delta T|$ correspond to the lipid domains containing GSM and the peak with higher $|\Delta T|$ values could be referred to lipid domains containing GSA. Linearity of $|\Delta T|(c)$ for the GSA-containing domains signs, in the simplest case, that the concentration of GSA in domains is directly proportional to GS content in the system. As to the GSM-containing domains, $\gamma > 1$ could be formally attributed to generation of additional membrane free volume comparing to one-mode dopant embedding. Besides, such supposition is in agreement with increase in the volume compressibility under GS sorption [23].

5.2. Mutual impact of the mechanisms of GS monomers and associates distribution into the lipid membrane

In our previous works, we considered dopants which only distribute to polar part of the lipid membrane [22] or to its non-polar part [32]. We also considered a case of two dopants distribution which caused changes in drug permeability of a dopant in the present of another one [6].

In the case of GS, the same dopant is able to distribute both to the polar part (surface) and to the non-polar part (interior) of the lipid membrane. Complex interrelations between hydrophilic and hydrophobic moieties of lipid membrane [33] makes mutual impact of the dopants with different types of localization possible. There are some examples of such non-direct hydrophilic-hydrophobic interactions in literature [34–36]. The systems considered in the present work are of especial interest because the same dopant modifies both membrane parts by two different mechanisms. As it is shown below, it could be mutual impact of the alternative embedding mechanisms that allows one to explain a number of unusual features of GS membranotropic action noted in Sec. 5.1.

To describe it in details, let us consider the membrane surface which consists of equal symmetric lipid cells [22]. As it was discussed in [6], a reason of the permeability changes in the case of two dopants is deformation of the lipid cells by the 1st dopant which impact their penetration by the 2nd dopant. Generally, deformation of the lipid cells influences on the GSM sorption not only via facilitation of their embedding into membrane (merely diffusion mechanism comprises that the permeability for GSM from water to lipid fraction would be changed whereas the permeability in opposite direction would remain unchanged). Additionally, a probability of a dopant binding to a membrane could change, which is defined by the depth of the potential well in the site of binding. The issue of the domination mechanism of sorption changes requires more studies and is out of the scope of the present work. However, general considerations remain the same and similar expressions could be obtained, only with different constants resulting from another shape of the interaction potential (yet essentially these constants should be defined experimentally). So, hereinafter we use the results obtained in [6] for simplicity and consider merely diffusion process.

As it was shown in [6], the membrane permeability P under deformation of the lipid cells has the form

$$P = P_0 + p_1\langle\sigma\rangle + p_2\langle\sigma^2\rangle, \qquad (4)$$

where σ is the deviation of the cell area from the initial (non-deformed) state. As it was noted in [6], its averaging over all the cells gives $\sigma = 0$ when the total membrane area keeps constant. So, the quadratic term should be taken into account, which is responsible for the disordering degree under constant average cell area.

Then, the influence of a dopant on the membrane melting temperature (ΔT) could be properly explained by emergence of effective lateral pressure, negative or positive, resulting in membrane stretching or contraction, correspondingly. So, the dopants with such mechanism of membranotropic action changes the total membrane area, therefore we could restrict ourselves to the linear term in Eq. (4). The value of σ is positive under membrane stretching (for the dopants that diminish T, i.e. $\Delta T < 0$) and is negative under membrane contraction (for the dopants that elevate T, i.e.

$\Delta T > 0$). In all the cases, it is proportional to ΔT and, therefore, to a dopant concentration. The value $p_1 = \frac{P_0}{s_0} \cdot \left(1 - \frac{U'(s_0)}{kT} s_0\right) > 0$ [6] because the potential $U(s_0)$ decreases with s_0.

Under the given dopant content, the equilibrium concentration of adsorbed dopant molecules, s, is generally proportional to the probability of their binding to membrane and ΔT_m is proportional to s. Using Eq. (3), we obtain $s = A_s c c^{\alpha}$ for GSM binding and $s = A_d c c^{\beta}$ for GSA binding in the case of their independent binding. Whereas in the case of conjunction caused by GSA impact on GSM sorption, we obtain for GSM:

$$s = A_s c^{\alpha} + \tilde{p}_1 A_s A_d c^{\alpha} c^{\beta}, \quad (5)$$

where c is GS concentration in the system; $\tilde{p}_1(c)$ is an analog of p_1 (Eq. (4)); A_s, A_d, α, β have the same sense as b and γ in Eq. (3).

Then melting temperature shift will be equal to

$$\Delta T = C_{T1} \cdot c^{\alpha} + C_{T2} \cdot c^{\beta} + C_{T12} \cdot c^{\alpha+\beta}, \quad (6)$$

where C_{T1}, C_{T2} and C_{T12} are constants related to A_s, A_d, $\tilde{p}_1$ and the constants which connect s and ΔT.

The exponents of the first two terms in Eq. (6) are less than 1, which is in line with Freundlich law (3). But if these terms are relatively small comparing to the third one (i.e. separate sorption of GSM and GSA is sufficiently lower than sorption of GSM in the presence of GSA), the main contribution is made by the third term, so

$$\Delta T \approx C_{T12} \cdot c^{\alpha+\beta}. \quad (7)$$

This dependence has exponent $\alpha+\beta$, which may be higher than 1 (in particular, it may be equal to 1.6 which was established from the experiment (Fig. 2), and describes mutual impact of different mechanisms of dopant embedding, or conjunction of these mechanisms.

Such conjunction could be involved to explain $|\Delta T|$ elevating in the GSA-containing lipid domains with GS concentration (Fig. 2, A). Such elevating manifests corresponding increase in the GSA concentration, i.e. GSA embedding in the vicinity of each other. It seems believable that probability of such self-assembly is much more higer than embedding of GSA into other sites of the membrane. It results to formation and growth of domains with high GSA concentration [4, 13]. However, a question arises, why the grows of this phase is limited? Why all newly-formed GSA does not embed in the same domains and this phase does not distribute over the whole membrane?

One can suppose that a neat membrane has not enough free volume to embed GSA into lipid tails region. So, they only get the opportunity to embed due to the free volume generated due to GSM sorption. Thus, reciprocal mechanism of hydrophilic-hydrophobic interaction takes place. In this case, GSA could occupy free volume generated on the microdomains boundaries (and nothing beyond that) and, therefore, GSA-phase would be limited by size (see Sec. 5.3).

When GS concentration is lower than the threshold (see Sec. 1), membrane free volume appears still insufficient to GSA formation and embedding. Reaching the threshold concentration results to formation of GSA lipid shells and their separation into a lipid phase with its own characteristic melting temperature.

5.3. On limitation of GSA size

Elevation of GS concentration in the system could result either in growth of GSA size or amount of GSA of the same size. As it was mentioned above, GSA formation becomes possible when there is enough free volume inside the membrane. Meanwhile, if below the threshold concentration there was insufficient amount of free volume even for GS dimer formation (Fig. 3), one can suppose that above the threshold GS dimer would not only fill the accessible free volume but cause its certain lack in the neighboring lipid cells (Fig. 5). This process could distribute involving further lipid cells until accessible free volume will over. Then GSA growth would be stopped. Thus, we obtain certain limitations on GSA size.

We assume GSA size to be related on GS concentration. Below, there are some considerations which would help us to estimate the size. It is known that lipids in membrane form hexagonal or quasi-hexagonal lattice [37], so the membrane surface could be roughly represented as a set of hexagonal lipid cells.

Then, the following denotes should be introduced:

s_0 is the area of an unfilled ("free") lipid cell which depends on GSM concentration;
s is the area of a lipid cell with a dopant embedded ("filled");

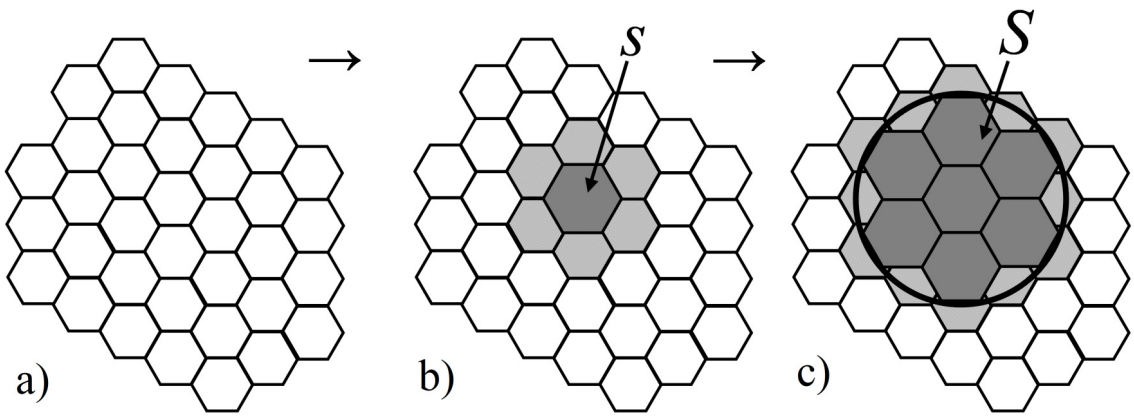

Fig. 5. A scheme of growth of GSA-containing domains: a — lipid cells without dopants ("free"); b — a lipid cell embedded with a dopant ("filled") and a layer of adjacent cells with disturbed properties ("disturbed"); c — dopant embedding involves further lipid cells. Patterns b–c show consecutive steps of GSA growth. Solid filling marks lipid cells with a dopant, hatching marks "disturbed" cells around the "filled" ones. S is the area of the lipid shell around GSA of maximal size; s is the area of a "filled" lipid cell.

s_c is the minimal area of lipid cell matching for GSA embedding (the same or less area has a 'disturbed' lipid cell next to the 'filled' by GSA of maximal size);

S is the area of cells involving in the lipid shells around GSA of maximal size.

Let us first consider the simplest case when GSA embedding just modifies one layer of "disturbed" cells (see Fig. 5) and GSA to be approximately round-shape.

Before dopant embedding, the "filled" cells had total area $\frac{S}{s} \cdot s_0$; the perimeter of the corresponding circle is $2\sqrt{\pi \cdot \frac{S}{s} \cdot s_0}$. The diameter of a "free" cell is $2\sqrt{\frac{s_0}{\pi}}$, so amount of such cell around the perimeter is $2\sqrt{\pi \cdot \frac{S}{s} \cdot s_0} / \; 2\sqrt{\frac{s_0}{\pi}} = \pi\sqrt{\frac{S}{s}}$. Their total area before dopant embedding is $\pi \cdot \sqrt{\frac{S}{s}} \cdot s_0$, therefore total area of all the cells that would be modified by GSA embedding is $\frac{S}{s} \cdot s_0 + \pi\sqrt{\frac{S}{s}} \cdot s_0$. After GSA embedding, the "filled" cells have area S. So, the "disturbed" cells have total area $\frac{S}{s} \cdot s_0 + \pi\sqrt{\frac{S}{s}} \cdot s_0 - S$ or $\left\{\frac{S}{s} \cdot s_0 + \pi\sqrt{\frac{S}{s}} \cdot s_0 - S\right\} / \; \pi\sqrt{\frac{S}{s}}$ per cell. Growth of GSA is stopped when this area becomes equal to s_c, so we obtain

$$\left(\frac{S}{s} \cdot s_0 + \pi\sqrt{\frac{S}{s}} \cdot s_0 - S\right) / \left(\pi\sqrt{\frac{S}{s}}\right) = s_c. \quad (8)$$

Moving further from our initial simplifications, we can introduce a constant k for accounting not circular GSA shape, non-ideality of lipid cells shape and packing, transfer from two-dimensional to three-dimensional description, etc.

So, we obtain:

$$S = k\pi^2 \frac{\left(1 - \frac{s_c}{s_0}\right)^2}{\frac{s}{s_0} + \frac{s_0}{s} - 2} s_0. \quad (9)$$

Here, s and s_c are constants which depends on the dimensions of the dopant embedded; s_0 is a free variable which depends on the generated free volume. For the above considerations, their values should be ranked as $s_c \le s_0 \le s$.

Analysis of (9) shows that $S \to 0$ if $s_0 \to s_c$, i.e. in the case when the size of "free" cell is too small that a dopant molecule is not able to embed. On the other hand, $S \to \infty$ if $s_0 \to s$, i.e. in the case when a dopant molecule freely embeds into a lipid cell without disturbing the next cell layer. The both of limiting cases seem quite naturally.

General shape of $S(s_0)$ following from Eq. (9) for $s = 1.05 s_c$, $k = 1$ is shown in Fig. 6. Since S corresponds to GSA of maximal size (under the above-mentioned assumptions), real pattern should comprise GSA size distribution (see insert in Fig. 6) where domains of different size face each other's boundaries.

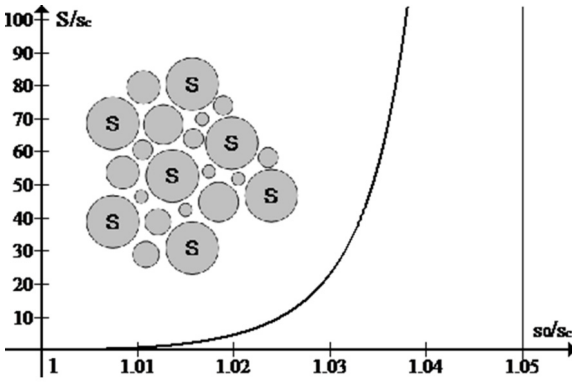

Fig. 6. GSA growth depending on relation s_0/s_c (Eq. 9) for $s = 1.05s_c$ and $k = 1$. The insert depicts GSA size distribution.

The above shows that GSA are formed, at least, under the impact of lipid media (or only therein) rather than embed independently from the water phase. Moreover, the model predicts increase of the maximal GSA size with increase of membrane free volume fraction. Indeed, as it was established experimentally, the thinner is lipid membrane (i.e. the higher is its free volume fraction) the larger is fraction of GS molecules involved in associate formation [4] which may be directly related to larger maximal size of GSA. The same phenomena explains higher GS sorption to the membranes with lower lipid ordering [15] and facilitation of GSA formation in the region of membrane phase transition [4]. Indeed, in all these cases, free volume fraction rises resulting to diminishing of the elastic component of lipid-lipid interactions [32] and, therefore, to facilitation of dopant embedding into the hydrophobic part of the membrane. In other words, increase in the free volume (both that inherent to neat membrane and that induced by dopants sorption) reduces contribution of the elastic component and thus actually shifts the equilibrium GSM $\longleftrightarrow$ GSA towards GSA formation.

Taking into account that the cooperative number of DMPC membrane under the experimental conditions reaches hundreds of lipid molecules [38] we should expect that GSA formation following the model developed would diminish it essentially due to great difference between "disturbed" and 'filled' lipid cells in the vicinity of GSA. Indeed, our DSC data evidence about significant decrease of the cooperative number just for GSA-containing domains (see Fig. 2, B). So, from structural viewpoint, the system considered is a two-dimension nanoemulsion composed of GSA-containing and GSM-containing microdomains which, in turn, are formed by characteristic sub-clusters (lipid shells of GSA and GSM) of the order of ten to hundred particles. Such structure, in particular, suggests that processes on the microdomains boundaries, including generation of free volume, would impact significantly on the system properties.

6. Conclusions

Model lipid membrane of hydrated DPPC in the presence of GS tend to separate into two types of lipid phases (microdomains) with different properties. There are two apparent reasons for such effect. First, it is the ability of GS to form associates. Unlike GS monomers, which localize in the vicinity of the hydrophilic membrane surface, the associates embed into the hydrophobic part membrane due to certain changes of physicochemical parameters under their formation, such as size enlargement, charge shielding, lipophilicity elevation, etc. The second reason is ability of the associates to embed close to each other, with growth of their local concentration inside the membrane. As a result, the monomer-containing lipid domains and the associates-containing domains occurs simultaneously which seems an appropriate reason of elevation of the membrane permeability reported in literature.

A set of unusual membranotropic effects of GS was observed experimentally, which allowed us to assume conjunction of alternative mechanisms of GS embedding into DPPC membrane. This conjunction consists in generation of additional free volume in the membrane which, on the one hand, causes a power-law concentration dependence of phase transition temperature for monomer-containing domains, where the exponent is higher than 1 and, on the other hand, facilitates embedding of GS associates and restricts their growth. The model developed shows that increase in non-selective membrane permeability which is believed to be main mechanism of GS antimicrobial action, could be a direct consequence of GS-induced non-homogeneity in lipid packing rather than pore formation. Additionally, the model explains a number of features of GS membrane interactions, namely

(1) the concentration threshold for formation of GSA-containing domains;

(2) a power-law concentration dependence of phase transition temperature for the

monomer-containing domains, where the exponent is higher than 1;

(3) elevation of the fraction of GS molecules involved in associate formation with membrane thinning;

(4) higher GS affinity to the membranes with lower lipid ordering;

(5) facilitation of GSA formation in the region of membrane phase transition, etc.

The model could be useful for interpretation and prediction of GS effect in various model and cell membranes.

References

1. J.Li, J.-J.Koh, S.Liu, R.Lakshminarayanan et al., *Front. Neurosci.*, **11**, 73 (2017).
2. G.Gause, M.Brazhnikova, *Nature*, **154**, 703 (1944).
3. H.Yonezawa, K.Okamoto, K.Tomokiyo et al., *J. Biochem.*, **100**, 1253 (1986).
4. S.Afonin, U.H.N.Durr, P.Wadhwani et al., *Top. Curr. Chem.*, **273**, 139 (2008).
5. K.Lohner, S.E.Blondelle, *Comb. Chem. High Throughput Screen.*, **8**, 241 (2005).
6. N.A.Kasian, O.V.Vashchenko, L.V.Budianska et al., *Biochim. Biophys. Acta-Biomembr.*, **1861**, 123 (2019).
7. L.H.Kondejewski, S.W.Farmer, D.S.Wishart et al., *J. Biol. Chem.*, **271**, 25261 (1986).
8. T.Kim, K.I.Lee, P.Morris et al., *Biophys. J.*, **102**, 1551 (2012).
9. M.Wenzel, M.Rautenbach, J.A.Vosloo et al., *mBio*, **9**, e00802-18 (2018).
10. M.Ashrafuzzaman, O.S.Andersen, R.N.McElhaney et al., *Biochim. Biophys. Acta-Biomembr.*, **1778**, 2814 (2008).
11. M.Ashrafuzzaman, *Membranes*, **11**, 247 (2021).
12. T.Abraham, E.J.Prenner, R.N.A.H.Lewis et al., *Biochim. Biophys. Acta-Biomembr.*, **1838**, 1420 (2014).
13. O.Babii, S.Afonin, A.Yu.Ishchenko et al., *J. Med. Chem.*, **61**, 10793 (2018).
14. S.Reiber, E.Strandberg, T.Steinbrecher et al., *Biophys. J.*, **106**, 2385 (2014).
15. E.J.Prenner, R.N.A.H.Lewis, L.H.Kondejewski et al., *Biochim. Biophys. Acta-Biomembr.*, **1417**, 211 (1999).
16. S.L.Grage, S.Afonin, S.Kara et al., *Front. Cell Dev. Biol.*, **4**, 65 (2016).
17. I.P.Sugar, A.P.Bonanno, P.L.-G.Chong, *Int. J. Mol. Sci.*, **19**, 3690 (2018).
18. M.Jelokhani-Niaraki, R.S.Hodges, J.E.Meissner et al., *Biophys. J.*, **95**, 3306 (2008).
19. C.McInnes, L.H.Kondejewski, R.S.Hodges et al., *J. Biol. Chem.*, **275**, 14287 (2000).
20. QtiPlot — Data Analysis and Scientific Visualisation [electronic resource]. URL: https://www.qtiplot.com.
21. H.M.F.Freundlich, *J. Phys. Chem. A.*, **57**, 385 (1906).
22. O.V.Vashchenko, N.A.Kasian, L.V.Budianska et al., *J. Mol. Liq.*, **275**, 173 (2019).
23. R.Krivanek, L.Okoro, R.Winter, *Biophys. J.*, **94**, 3538 (2008).
24. G.W.Feigenson, *Biochim. Biophys. Acta*, **1788**, 47 (2009).
25. W.Diakowski, L.Ozimek, E.Bielska, S.Bem et al., *Biochim. Biophys. Acta*, **1758**, 4 (2006).
26. Chemdraw 3d free download social advice [electronic resourse]: URL: https://www.softadvice.informer.com/Chemdraw_3d_Free_Download.html.
27. A.O.Sadchenko, O.V.Vashchenko, A.Yu.Puhovkin et al., *Biophysics*, **62**, 570 (2017).
28. K.N.Belosludtsev, N.V.Penkov, K.S.Tenkov, *Chem.-Biol. Interact.*, **299**, 8 (2019).
29. W.K.Subczynski, M.Pasenkiewicz-Gierula, J.Widomska et al., *Cell Biochem. Biophys.*, **75**, 369 (2017).
30. R.N.McElhaney, *Chem. Phys. Lipids*, **30**, 229 (1982).
31. G.Neunert, J.Tomaszewska-Gras, M.Gauza-Wlodarczyk et al., *Appl. Sci.*, **13**, 6219 (2023).
32. R.Ye.Brodskii, O.V.Vashchenko, *Func. Mater.*, **28**, 525 (2021).
33. M.S.Giammarinaro, S.Micciancio, *Mol. Cryst. Liq. Cryst.*, **76**, 35 (1981).
34. M.Ricci, R.Oliva, P.Del Vecchio et al., *Biochim. Biophys. Acta*, **1858**, 3024 (2016).
35. G.S.S.Ferreira, D.M.Perigo, M.J.Politi et al., *Photochem. Photobiol.*, **63**, 755 (1996).
36. N.Toyran, F.Severcan, *Spectroscopy*, **16**, 399 (2002).
37. T.Heimburg, *Biochim. Biophys. Acta.*, **1415**, 147 (1998).
38. N.A.Kasian, O.V.Vashchenko, L.V.Budianska et al., *J. Therm. Anal. Calorim.*, **136**, 795 (2019).